Fermi National Accelerator Laboratory

FN-536

Study of Separators Using Numerical Simulations*

Fady A. Harfoush and King-Yuen Ng
Fermi National Accelerator Laboratory
P.O. Box 500
Batavia, Illinois 60510

March 1990

* Presented at the Los Alamos Conference on Computer Codes and the Linear Accelerator Community, Los Alamos, New Mexico, January 22-25, 1990.

STUDY OF SEPARATORS USING NUMERICAL SIMULATIONS

Fady A. Harfoush and King-Yuen Ng

Fermi National Accelerator Laboratory
Batavia, IL 60510

March, 1990

1 Introduction

Electrostatic separators are placed in the Tevatron to control long range beam-beam effects. The effect these separators will have on the impedance is calculated using the 3-D time domain code MADIA-T3, the 2-D eigenmodes solver URMEL-T and the 3-D eigen solver E31 [2, 3]. The model considers two parallel perfectly conducting plates placed in a circular cavity. No charges or potentials are placed on the surfaces of the plates. The model does not incorporate the cables powering the separators. These simplifications are necessary because of the code limitations. Still the simplified model should gives us a good understanding of the impedances.

The integrated wake force components governing our geometry are given in cylindrical coordinates[1] as:

$$F_z(s) = \sum_{m=0}^{\infty} eI_m W'_m(s) r^m \cos m(\theta - \phi) \quad (1)$$

$$F_\perp(s) = \sum_{m=1}^{\infty} eI_m W_m(s) m r^{m-1} [\hat{r} \cos m(\theta - \phi) - \hat{\theta} \sin m(\theta - \phi)] + F_\perp^o(s) \quad (2)$$

where e is the charge of the test particle, $s = z_o - z$ is the longitudinal distance the test particle is lagging behind, r and a are respectively the

offsets of the test particle and source particle. The multipole coefficients of the point source are $I_m = qa^m$, where q is the charge of the source. $W_m(s)$ is the transverse wake function or wake potential in the m-th multipole and W'_m is the corresponding longitudinal wake function. Here the wake forces are computed at $\theta = \phi$.

The problem geometry is shown in Fig. 1. The length of the circular cavity is 3.11 m and the radius of the cavity is 0.18 m. Because of the problem symmetry, the $m = 0$ component represented by $F_\perp^o(s)$ in Eq. (2) is zero. To obtain results as accurate as possible and because of the limitations on the size of the problem we can run on our VAX/8650, a grid mesh of 16 x 19 x 312 is selected corresponding to half the problem geometry. We have also computed the longitudinal wake force for a sufficient long time, equivalent to 15 m, to pick up two reflections across the ends of the separators.

2 Modeling Half the Geometry

An efficient way to do these calculations is to consider half of the geometry only. One should however proceed with caution. The beam can still be placed at the center axis of the geometry which is now in the symmetry plane at the extreme left boundary of Fig. 1b. The boundary condition $E_{tangential} = 0$ at the symmetry plane results in an image current traveling in the opposite direction. This does not make sense since now each half of the beam is traveling in opposite directions. The boundary condition $H_{tangential} = 0$ leads to the proper behavior. For this latter case, the transverse wake force will be non zero. This is the repulsion force from half of the current image on the other half. Since each half of the beam experiences a similar force but in opposite direction, the resulting net transverse force on the whole current is zero.

By offseting the beam we can use either condition. A simple calculation shows that the condition $E_{tangential} = 0$ with $r = a$ results in the following equations:

$$F_z(s) = \sum_{m=0}^{\infty} eqW'_m(s)a^{2m} + \sum_{m=0}^{\infty} eqW'_m(s)(-1)^{m+1}a^{2m} \qquad (3)$$

$$F_\perp(s) = \sum_{m=1}^{\infty} eqW_m(s)ma^{2m-1} + \sum_{m=1}^{\infty} eqW_m(s)m(-1)^{m+1}a^{2m-1} \qquad (4)$$

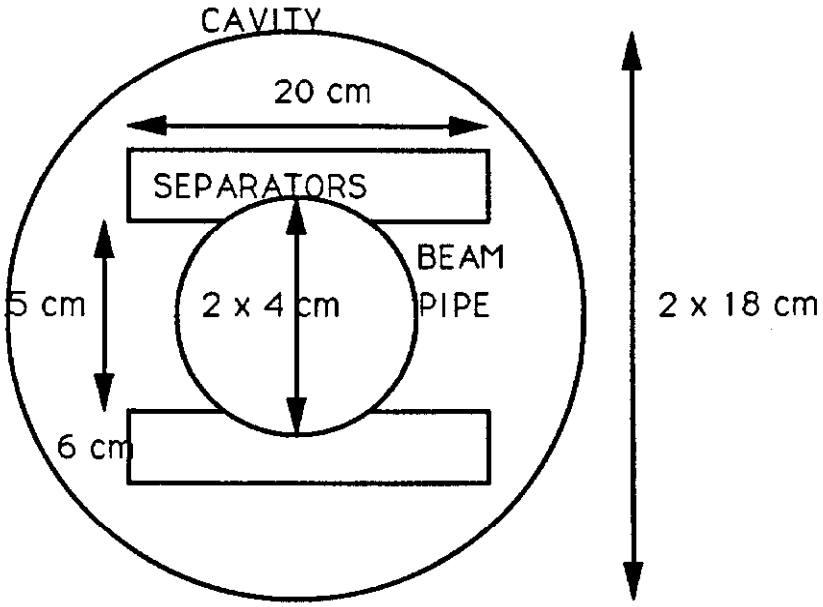

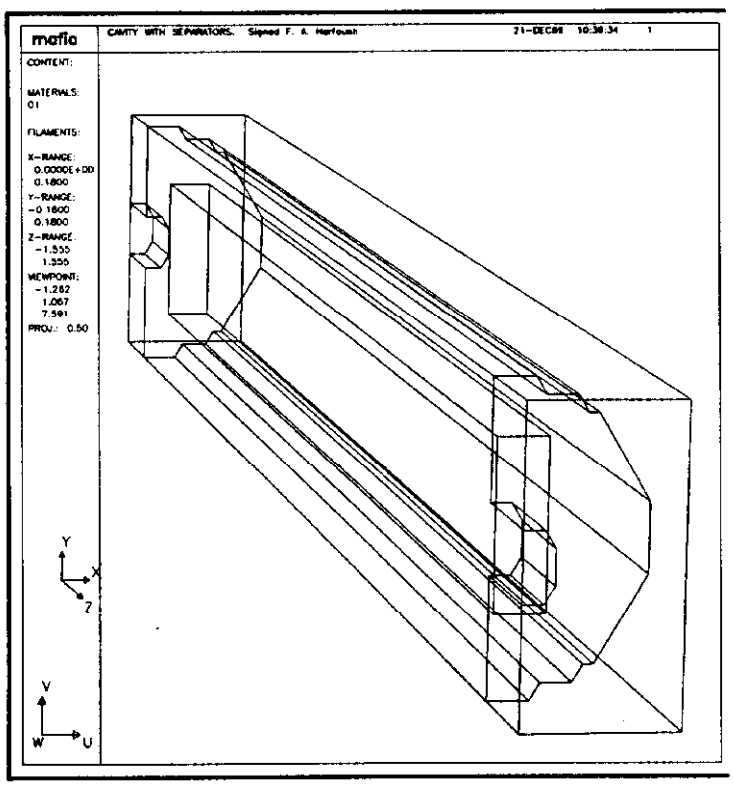

Figure 1: Problem geometry

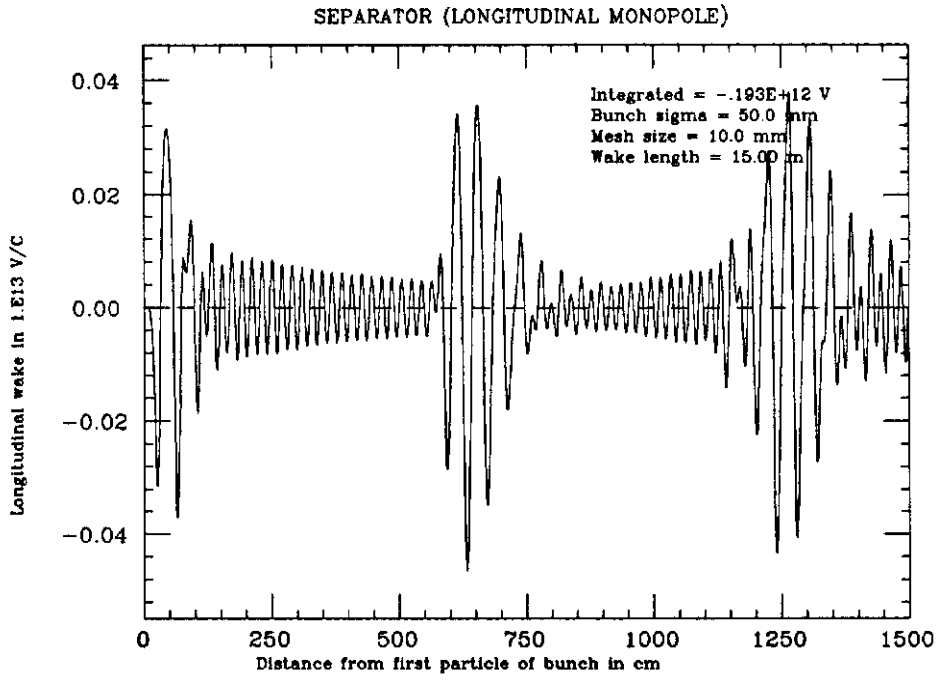

Figure 2: Longitudinal monopole

For the longitudinal or transverse wake we only have odd modes $1, 3, 5, \cdots$ Similarly, the condition $H_{tangential} = 0$ results in only even modes $0, 2, 4, 6, \cdots$ It should be noted that when extracting the dipole wake potential from the total wake force (assuming contribution from higher poles to be negligible) the final result should be divided by two.

Using half the geometry enables us to have more mesh points and therefore better resolution. The other main advantage is that less modes are calculated in the total wake force and therefore less error is involved in extracting a monopole, or a dipole.

3 Longitudinal Wakes

The longitudinal wake is calculated at the beam offset which is equal to one cell (0.012 m) in this case. The monopole part of the wake, shown in Fig. 2 is calculated with $H_{tang.} = 0$ at the symmetry plane. Also shown in Fig. 3 is the corresponding real and imaginary parts of the impedance .

It is noted from Fig. 2 the spatial distance between the two repeating high oscillations correspond to twice the length of the structure (2×3.1 m) which is equivalent to the time necessary for a wake to travel up and down the structure.

A similar calculation of the monopole longitudinal wake at the beam pipe

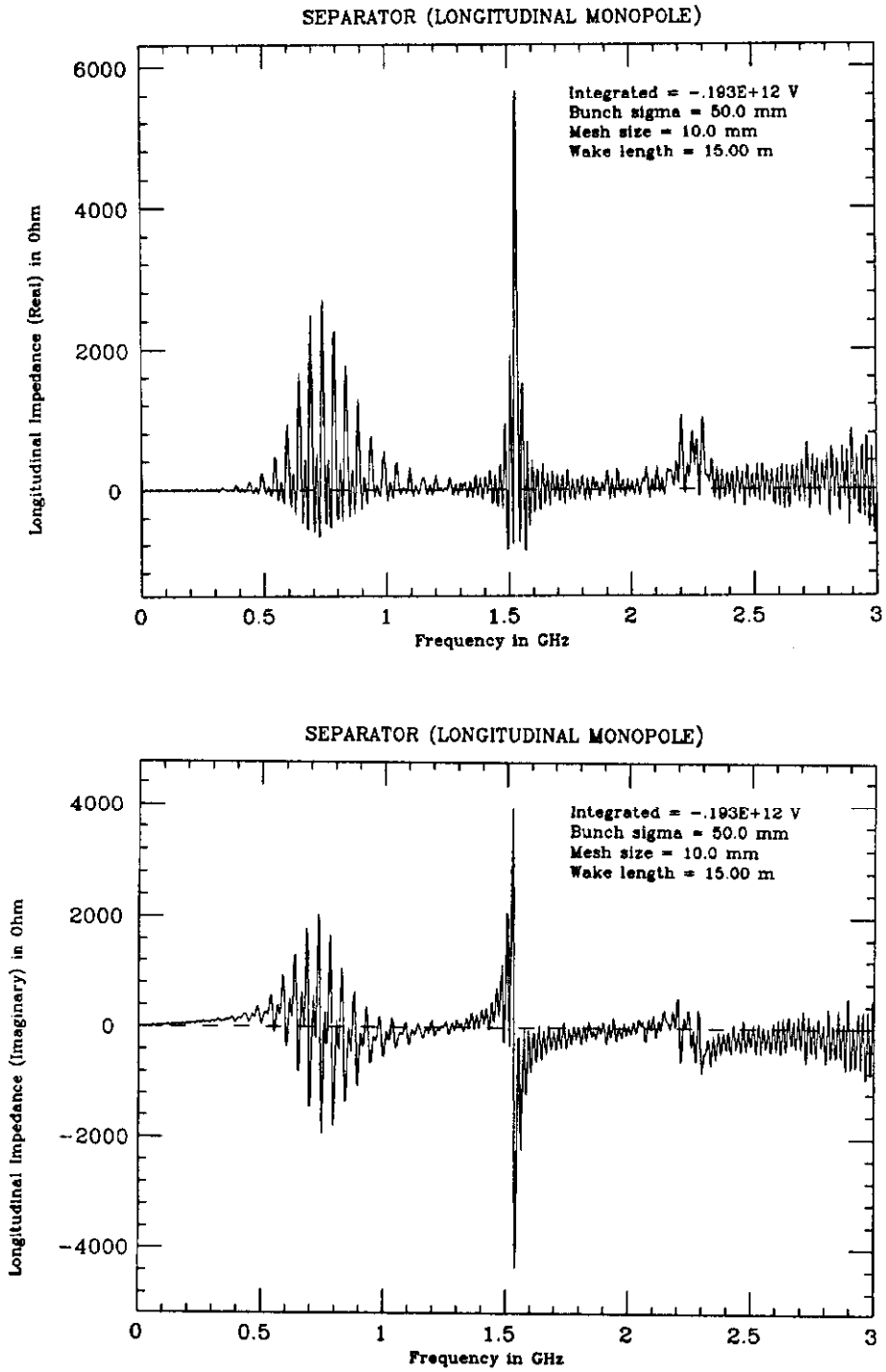

Figure 3: Real and imaginary parts of the longitudinal impedance

(r = 4 cm) instead of the beam axis gave undistinguishable results and are therefore not presented. This calculation basically shows that contributions from higher order multipole are small and the level of noise error from a smooth beam pipe is also small.

3.0.1 The Fourier Transform

Since impedance is obtained by taking the Fourier transform of the wake, it is important where one truncates the wake. A truncation at a point in the wake other than zero and with a smaller look-up window will lead to more noise in the output because of the sinc like behavior. Such a behavior is shown in Fig. 4 where the wake is truncated at 12.5 m instead of 15 m. This figure should be compared with Fig. 3.

One should also consider two other important factors. The beam pipe radius will set the cut-off frequency for the propagating modes. In our model the beam pipe radius is set at 4 cm. The corresponding lowest cutoff frequency is 2.87 GHz. Modes in the cavity with frequency greater than the beam pipe cutoff frequency will not be totally trapped and the Q factor for that mode will be much lower. Therefore high Q resonant modes will only be present up to 2.87 GHz. Also because we are using a gaussian bunch distribution of finite length, the impedance is the Fourier transform of the wake divided by the Fourier transform of the bunch distribution. For a gaussian bunch this transform has the form of:

$$exp - \left[\frac{1}{2}\left(\frac{\omega}{\sigma_\omega}\right)^2\right]$$

where $\sigma_\omega = \frac{c}{\sigma_l}$. For a bunch length of $\sigma_l = 5$ mesh sizes in the z-direction or 5 cm in our case, the above exponential will have a value of < 0.05 for a frequency $f < 2.33$ GHz. A division by small numbers will introduce more uncertainties in the result. The impedance spectrum should therefore not be trusted beyond 2.33 GHz.

4 Transverse Wakes

The transverse dipole is computed at the beam offset by imposing the boundary condition $E_{tangential} = 0$. Results are shown in Figs 5 and 6. It is also

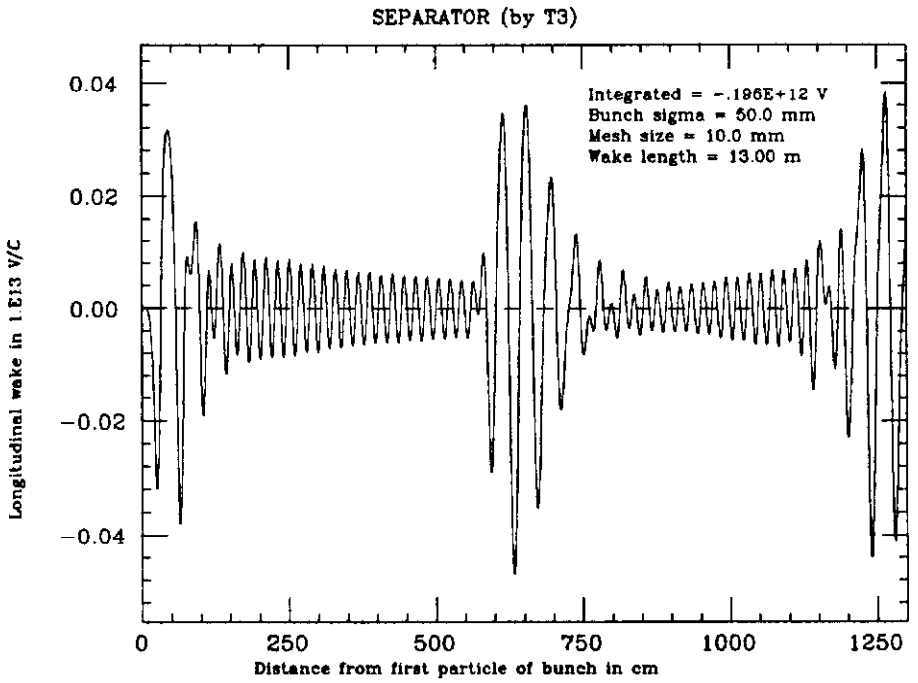

Figure 4: Longitudinal monopole for 12.5m

possible to calculate the transverse dipole from the longitudinal dipole by integrating this latter. Results obtained are similar to the results in Fig 5 and are not shown here.

5 The 2-D Approximate Solution

In many cases a 2-D approximation, assuming cylindrical symmetry of the 3-D problem, should give us a good preliminary insight as to the physics of the problem. Here we approximate our 3-D problem by coaxial guides assuming the separators to have cylindrical symmetry as shown in Fig. 7. It is now possible to calculate the eigenmodes of this structure using the eigenmode solver URMEL-T. The resonant shunt impedances are shown in Fig. 8.

These results depict the same behavior as obtained from MAFIA-T3. In both cases, T3 and URMEL-T, the cavity is excited by a beam traveling along its axis. Also, results of URMEL-T do take in consideration the transit time effect as the beam crosses the cavity structure.

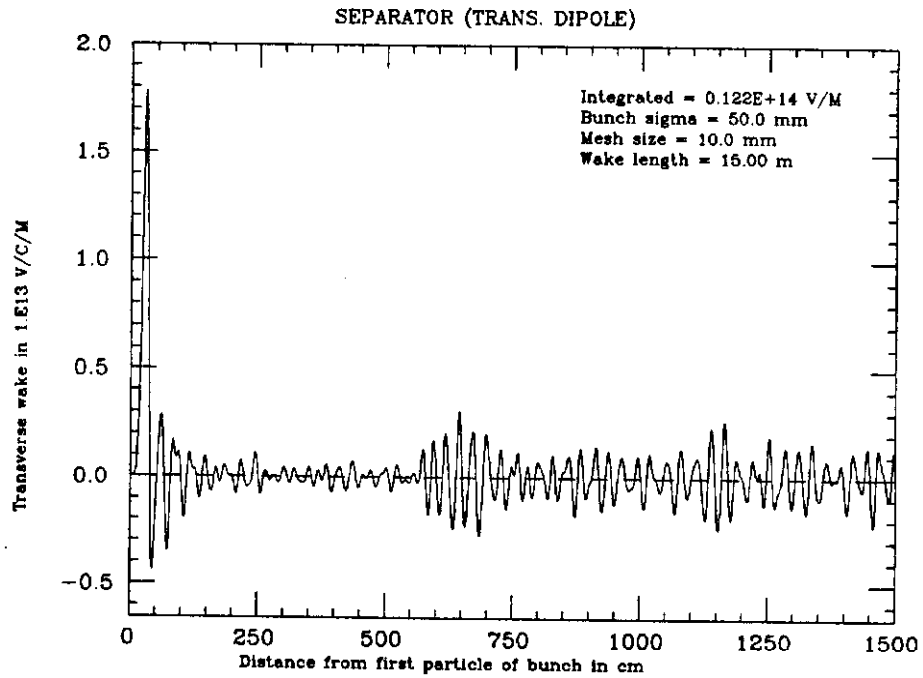

Figure 5: Transverse dipole wake

6 Physical Interpretation

The spectrum of the longitudinal impedance show three high Q resonances modulated by a broader band impedance. These high Q impedances located at $\sim$ 7 MHz, $\sim$ 1.5 GHz and $\sim$ 2.3 GHz can be attributed to the first three resonant modes of a cavity like structure of radius 18 cm. These resonant modes are modulated by a broader band impedance due to a transmission line effect.

A simple calculation of an open ended transmission line shows that propagating modes occur at $f = 54.5m$ MHz ($m = 1, 2, \cdots$) where the length of the transmission line is set equal to 2.75 m. The cavity effect is set by the radius of the cavity, 18 cm in this case, while the Q of the cavity is set by the cavity geometry. The resonant frequency for the first three TM modes are given by $f_{010} = 637$ MHz, $f_{020} = 1462.6$ MHz and $f_{030} = 2295$ MHz. The cavity and transmission line effects are clearly marked in Fig. 9.

The cavity high Q resonant frequencies together with the transmission line frequencies explain the shape of the impedance spectrum we observe.

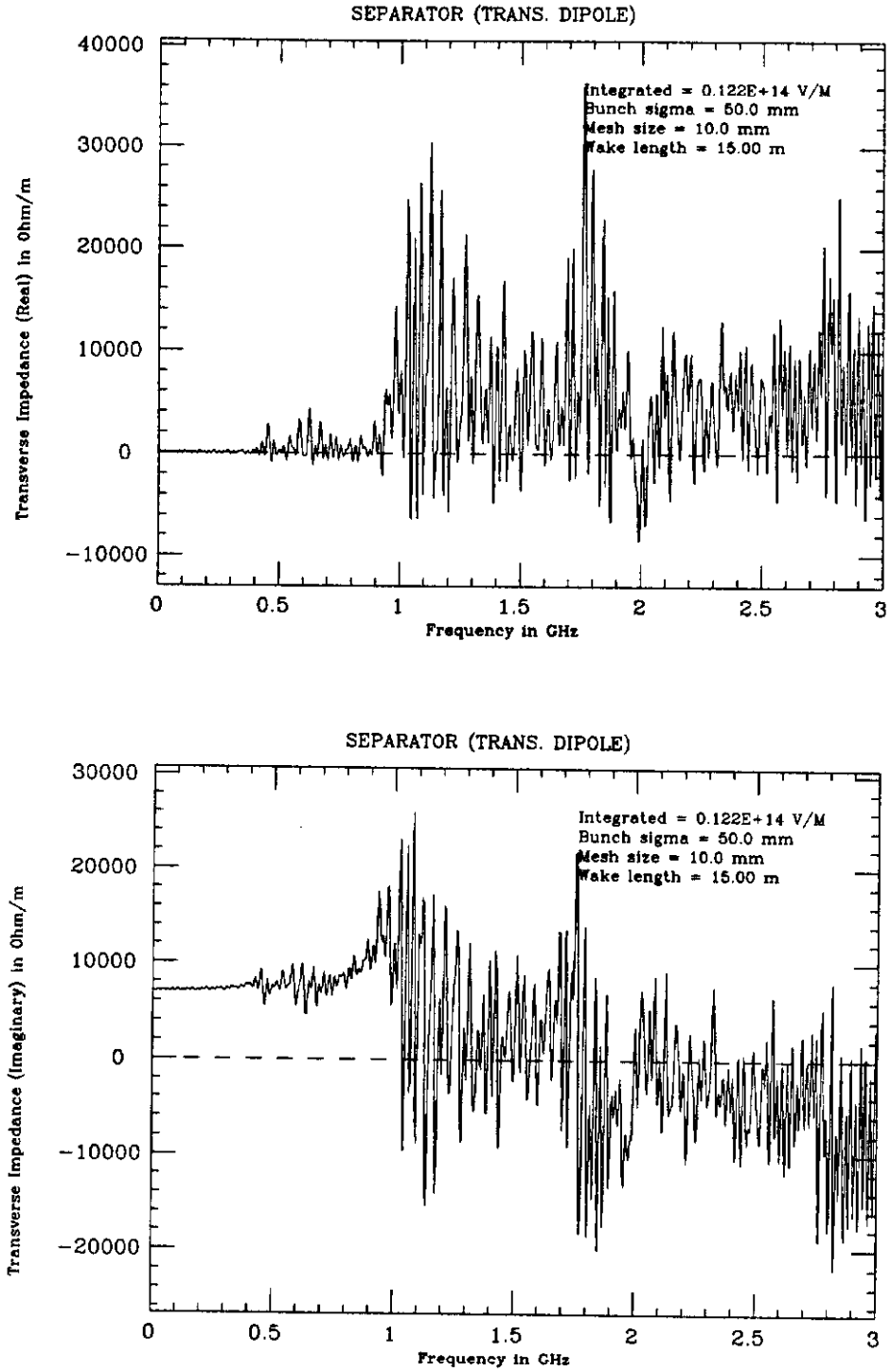

Figure 6: Real and imaginary parts of the transverse impedance

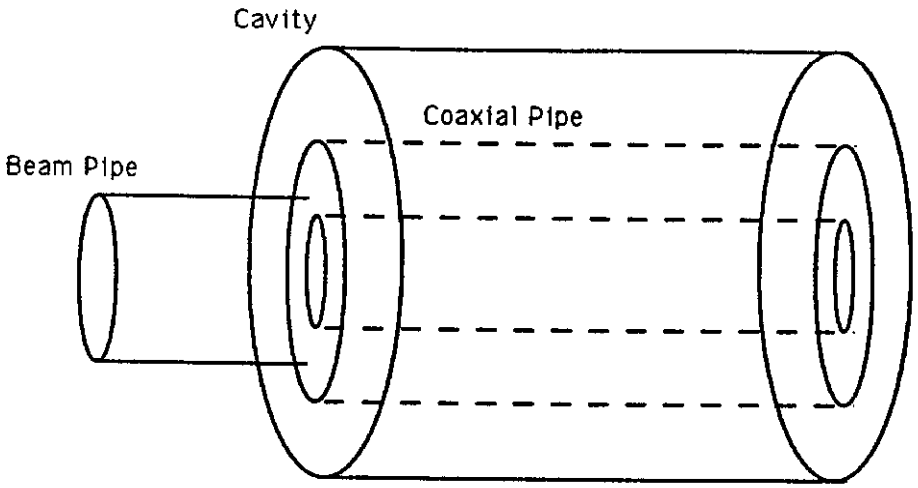

Figure 7: The 2-D coaxial guides model

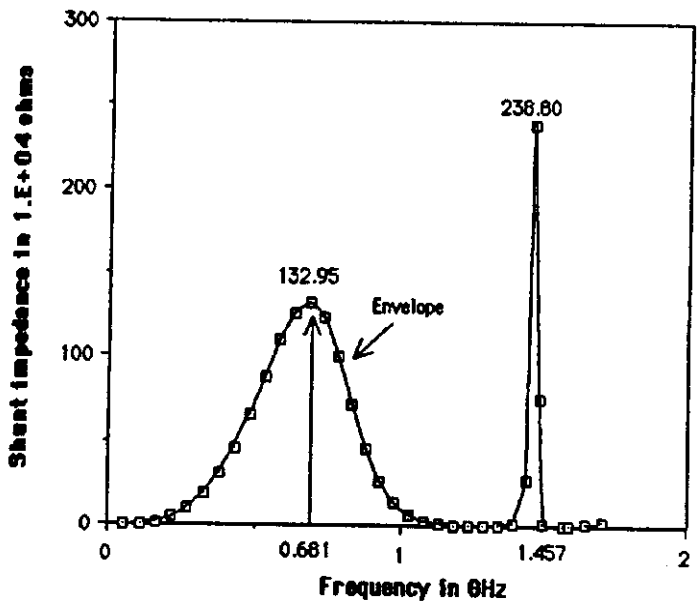

Figure 8: Resonant shunt impedances as obtained from URMEL-T

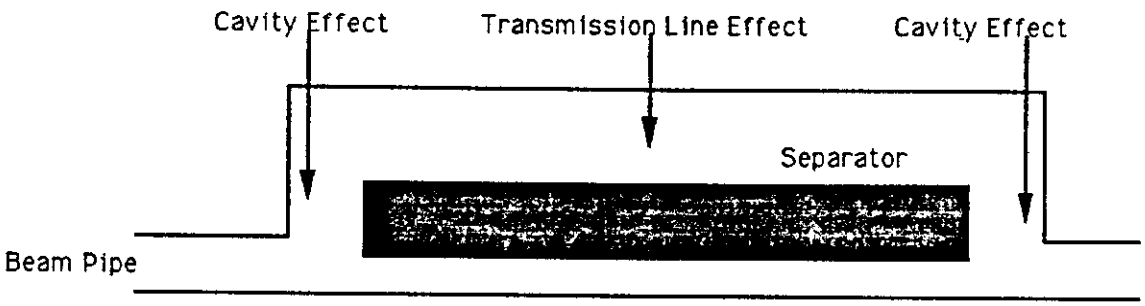

Figure 9: Mark-up of the cavity and transmission line effects

7 Cavity and Transmission Effects

To further test our theory and from a pedagogical point of view we did the following study. We selected different models where the transmission line effect or the cavity effect is enhanced. Results are shown in Fig. 10. Here we are interested in the relative amplitude of the shunt impedances and not their absolute values. For this reason the shunt impedance magnitudes in Fig. 10 have been ommitted and only the relative amplitudes are shown. The change in the initial frequency (28, 29, and 35 MHz) is due to the change in the effective transmission line length seen in each structure.

The first three models (a,b,c) is where the transmission line effect is dominant. This is seen by the relative peak in the resonant cavity mode. Because here the transmission line of length 2.57 m is short ended and is resonant, modes will occur at $f = 29.18(2m-1)$ MHz ($m = 1, 2\cdots$). It can also be shown for a short ended transmission line impedance versus frequency decays as $(2m-1)^{-\frac{1}{2}}$. Such a decay is also depicted in the URMEL-T results. The last two cases (d,e) are such that now the cavity effect is enhanced relative to the transmission line effect.

Finally a 3-D eigenvalue solver E31 result is shown in Fig. 11. Again result shows a resonant impedance at $\sim$ 700 MHz. However the presence of

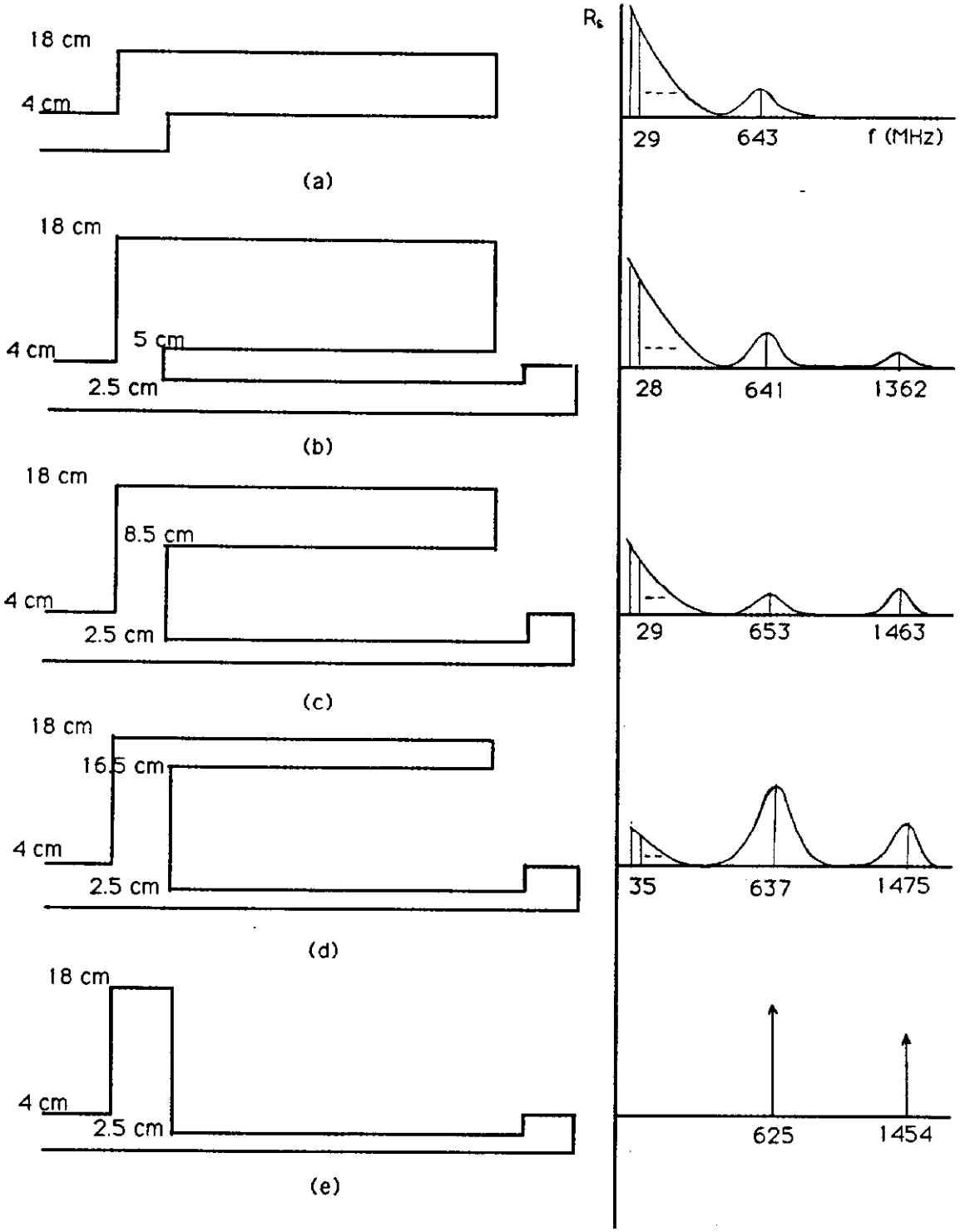

Figure 10: Enhancing cavity effects and transmission effects

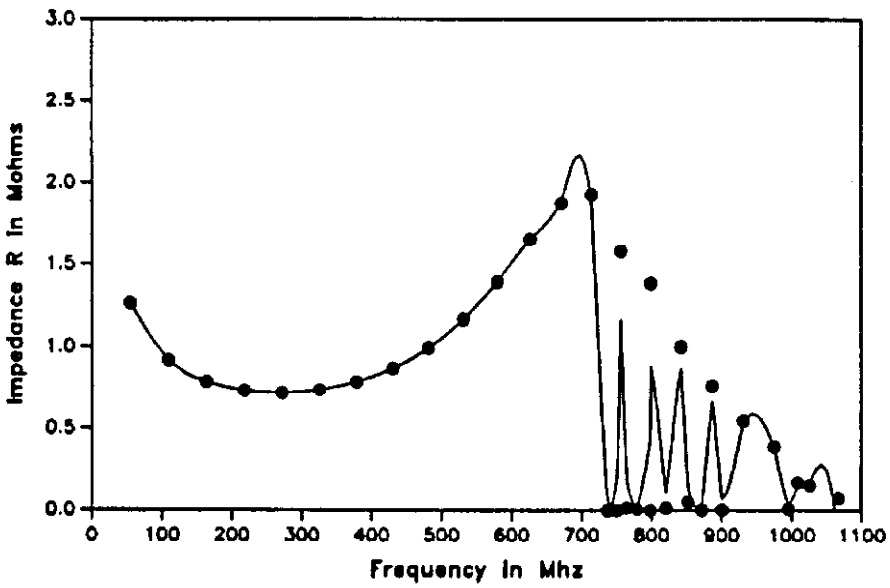

Figure 11: E31 results

many other close modes makes it hard to decide which one is a good mode or not.

8 CONCLUSIONS

This is our first attempt to model and study the effect of separators. It is clear from both the time domain MAFIA-T3 (3-D) results and the frequency domain 2-D URMEL-T results that three resonant impedances exist around $\sim$ 680MHz $\sim$ 1500 MHz and $\sim$ 2300 MHz. These modes correspond to the first three resonant TM modes f_{010}, f_{020} and f_{030} of the cavity like structure formed by the plates and the inner walls of radius 18cm. The frequencies are set by the radius of the cavity while the Q of the resonance depends on how narrow the cavity gap is. These resonant modes are modulated by a broader impedance spectrum corresponding to a transmission line effect. Initial results with the 3-D eigen mode solver E31 suggests the same behavior. However, because of the high number of close modes computed, it is difficult to draw a final conclusion.

Recent experimental results have also suggested a similar spectrum for the longitudinal impedance. We hope to have a full comparison of our numerical results and experimental results in the very near future.

References

[1] Alexander W. Chao, *SLAC-PUB-2946*, June 1982.

[2] T. Weiland, Particle Accelerators, **15**, 245 (1984).

[3] Mafia User Guide, DESY, LANL and KFA, May 3, 1988.